shock motion magnitude and phase angle have been deduced. A simplified approximate theory is also derived and the results compared to numerical data.

References

[1] Ashley, H., "On the Role of Shocks in the Sub-Transonic Flutter Phenomena," *Proceedings of AIAA Structural Dynamics Conference,* St. Louis, Mo., 1979.

[2] Williams, M.H., "Unsteady Thin Airfoil Theory for Transonic Flows with Embedded Shocks," Princeton University, MAE Rept. 1376, 1978.

[3] Seebass, A.R., Yu, N.J., and Fung, K.Y., "Unsteady Transonic Flow Computations," *Unsteady Aerodynamics AGARD Conference Proceedings,* No. 227, 1977.

[4] Nixon, D., "Notes on the Transonic Indicial Method," *AIAA Journal,* Vol. 16, June 1978, pp. 613-616.

[5] Tobak, M., "On the Use of the Indicial Function Concept in the Analysis of Unsteady Motions of Wings and Wing-Tail Configurations," NACA Rept. 1188, 1954.

[6] Ballhaus, W.F. and Goorjian, P.M., "Implicit Finite Difference Computations of Unsteady Transonic Flows Including the Effect of Irregular Shock Motions," *AIAA Journal,* Vol. 15, Dec. 1977, pp. 1728-1735.

Analytical Description of the Complete Turbulent Boundary-Layer Velocity Profile

David L. Whitfield*
ARO, Inc., Arnold Air Force Station, Tenn.

Nomenclature

a = parameter in Eq. (8)
b = parameter in Eq. (8)
$\bar{c}_f$ = local incompressible skin friction coefficient, $2\bar{\tau}_w/\bar{\rho}\bar{u}_e^2$
$\underline{p}$ = static pressure
$\overline{Re_\theta}$ = $\bar{\rho}\bar{u}_e\bar{\theta}/\bar{\mu}$
u = mean velocity in the x direction
$\bar{u}_\tau$ = $(\bar{c}_f/2)^{1/2}\bar{u}_e$
$\bar{u}^+$ = $\bar{u}/\bar{u}_\tau$
$\bar{u}_i^+$ = inner solution for $\bar{u}^+$
$\bar{u}_0^+$ = outer expression for $\bar{u}^+$
x = coordinate along body surface
y = coordinate normal to body surface
$\bar{y}^+$ = $\bar{u}_\tau\bar{\rho}\bar{y}/\bar{\mu}$
β = $(\bar{\delta}^*/\bar{\tau}_w)(d\bar{p}/d\bar{x})$
$\bar{\delta}^*$ = equivalent incompressible boundary-layer displacement thickness, $\bar{\delta}^* = \int_0^\infty [1-(\bar{u}/\bar{u}_e)]\,d\bar{y}$
$\bar{\theta}$ = equivalent incompressible boundary-layer momentum thickness, $\bar{\theta} = \int_0^\infty \frac{\bar{u}}{\bar{u}_e}[1-(\bar{u}/\bar{u}_e)]\,d\bar{y}$
μ = molecular viscosity
ρ = density
$-\rho\overline{u'v'}$ = Reynolds stress
τ = total shear stress

Subscripts

e = boundary-layer edge value
w = wall value

Superscript

$\bar{(\ )}$ = equivalent incompressible value

Presented as Paper 78-1158 at the AIAA 11th Fluid and Plasma Dynamics Conference, Seattle, Wash., July 10-12, 1978; submitted Aug. 1, 1978; revision received Feb. 13, 1979. Copyright © American Institute of Aeronautics and Astronautics, Inc., 1978. All rights reserved.

Index category: Boundary Layers and Convective Heat Transfer—Turbulent.

*Supervisor, Analysis Section, 16T/S Projects Branch, Propulsion Wind Tunnel Facility. Member AIAA.

Introduction

A COMMONLY used analytical representation of turbulent boundary-layer velocity profiles is that of Coles.[1] Coles' velocity profile expression is valid from outside the buffer layer to the edge of the boundary layer, and depends on the skin friction, boundary-layer thickness, and the profile parameter Π. A new analytical representation of two-dimensional turbulent boundary-layer velocity profiles is presented in this Note that is valid for smooth impermeable walls for the entire domain $0 \le y < \infty$. The expression is a linear combination of two trigonometric functions that depend on the inner variable $\bar{y}^+$, the outer variable $\bar{y}/\bar{\theta}$, and the parameter's skin friction, shape factor, and Reynolds number based on momentum thickness. The derivation of this expression is outlined and examples presented to illustrate the quality of agreement with experimental data. The application of this expression is simple and straightforward, and the steps are summarized in Table 1.

Analytical Development

The analytical expression is required to have the following properties: 1) recover the solution developed in Ref. 2 for the inner region, i.e., $\bar{y}^+ < O(10^2)$; 2) approach the proper limiting value of $\bar{u}^+ \to \bar{u}_e^+$ (or $\bar{u}/\bar{u}_e \to 1$) as $\bar{y} \to \infty$; and 3) recover the velocity profiles similar to those correlated by von Doenhoff and Tetervin[3] away from the wall in the outer variable $\bar{y}/\bar{\theta}$. The first requirement comprises the inner solution denoted as $\bar{u}_i^+$; the second and third requirements comprise the outer solution denoted as $\bar{u}_0^+$. A composite solution $\bar{u}^+$ is taken as

$$\bar{u}^+ = \bar{u}_i^+ + \bar{u}_0^+ \tag{1}$$

The derivation of the inner solution is given in detail in Ref. 2. The significance of the results of Ref. 2 is that a description of mean turbulence quantities in the inner region was obtained in exceedingly simple mathematical form. This is indicated by Fig. 1 and the corresponding inner solutions for the velocity, Reynolds stress, turbulence production, and direct dissipation of mean flow energy given, respectively, as

$$\bar{u}_i^+ = \frac{1}{0.09}\tan^{-1}(0.09\bar{y}^+) \tag{2}$$

$$\frac{-\overline{u'v'}}{\bar{u}_\tau^2} = \frac{(0.09\bar{y}^+)^2}{1+(0.09\bar{y}^+)^2} \tag{3}$$

$$\frac{-\overline{u'v'}}{\bar{u}_\tau^2}\frac{d\bar{u}_i^+}{d\bar{y}^+} = \left(\frac{0.09\bar{y}^+}{1+(0.09\bar{y}^+)^2}\right)^2 \tag{4}$$

$$\left(\frac{d\bar{u}_i^+}{d\bar{y}^+}\right)^2 = \left(\frac{1}{1+(0.09\bar{y}^+)^2}\right)^2 \tag{5}$$

Further comments of these inner region results and comparisons with experiment are given in Ref. 5.

In contrast to $\bar{u}_i^+$, $\bar{u}_0^+$ does not have a theoretical background. The outer variable is taken as $\bar{y}/\bar{\theta}$ and $\bar{u}_0^+$ is

Table 1 Procedure for computing turbulent boundary-layer velocity profiles

Step	Requirement	Comment
1)	$\bar{H}$, $\bar{u}_e^+$, and $\overline{Re}_\theta$ are inputs	$\bar{u}_e^+ = (2/\bar{c}_f)^{1/2}$
2)	Compute $\frac{\bar{u}}{\bar{u}_e}(2) = 1.723\left(1+\frac{50}{\overline{Re}_\theta}\right)e^{-0.6\bar{H}}$	$\frac{\bar{u}}{\bar{u}_e}\left(\frac{\bar{y}}{\bar{\theta}}\right)$ at $\frac{\bar{y}}{\bar{\theta}}=2$
3)	Compute $\frac{\bar{u}}{\bar{u}_e}(5) = 0.87 + 0.08e^{-2.6(\bar{H}-1.95)^2}$	$\frac{\bar{u}}{\bar{u}_e}\left(\frac{\bar{y}}{\bar{\theta}}\right)$ at $\frac{\bar{y}}{\bar{\theta}}=5$
4)	Compute $g(2) = \left(\frac{\bar{u}}{\bar{u}_e}(2) - \frac{1}{0.09\bar{u}_e^+}\tan^{-1}\frac{0.18\overline{Re}_\theta}{\bar{u}_e^+}\right)\Big/\left(1-\frac{\pi}{0.18\bar{u}_e^+}\right)$	$g\left(\frac{\bar{y}}{\bar{\theta}}\right)$ at $\frac{\bar{y}}{\bar{\theta}}=2$
5)	Compute $g(5) = \left(\frac{\bar{u}}{\bar{u}_e}(5) - \frac{1}{0.09\bar{u}_e^+}\tan^{-1}\frac{0.45\overline{Re}_\theta}{\bar{u}_e^+}\right)\Big/\left(1-\frac{\pi}{0.18\bar{u}_e^+}\right)$	$g\left(\frac{\bar{y}}{\bar{\theta}}\right)$ at $\frac{\bar{y}}{\bar{\theta}}=5$
6)	Compute $b = \ell n\left(\frac{\tanh^{-1}[g^2(2)]}{\tanh^{-1}[g^2(5)]}\right)\Big/\ell n\left(\frac{2}{5}\right)$	$\tanh^{-1}z = \frac{1}{2}\ell n\left(\frac{1+z}{1-z}\right)$
7)	Compute $a = \tanh^{-1}[g^2(2)]/2^b$	$\tanh z = \frac{e^{2z}-1}{e^{2z}+1}$
8)	$\bar{u}^+ = \frac{1}{0.09}\tan^{-1}(0.09\bar{y}^+) + \left(\bar{u}_e^+ - \frac{\pi}{0.18}\right)\tanh^{1/2}\left[a\left(\frac{\bar{y}}{\bar{\theta}}\right)^b\right]$	$\frac{\bar{u}}{\bar{u}_e} = \frac{\bar{u}^+}{\bar{u}_e^+} = \frac{u}{u_e}$ $\bar{y}^+ = \frac{\overline{Re}_\theta}{\bar{u}_e^+}\cdot\frac{\bar{y}}{\bar{\theta}}$

derived empirically as follows. Note from Eq. (2) that as $\bar{y}^+ \to \infty$, $\bar{u}_i^+ \to \pi/0.18$. Therefore, according to Eq. (1), for $\bar{u}^+$ to have the proper limiting value of $(2/\bar{c}_f)^{1/2}$ as $\bar{y}\to\infty$, $\bar{u}_0^+$ must behave as

$$\bar{u}_0^+ \to \left[\left(\frac{2}{\bar{c}_f}\right)^{1/2} - \frac{\pi}{0.18}\right]$$

as $\bar{y}\to\infty$. Furthermore, because $\bar{u}_i^+$ gives the desired result for small $\bar{y}$, $\bar{u}^+$ must behave as $\bar{u}_0^+ \to 0$ as $\bar{y}\to 0$. Therefore, the form

$$\bar{u}^+ = \frac{1}{0.09}\tan^{-1}(0.09\bar{y}^+) + \left[\left(\frac{2}{\bar{c}_f}\right)^{1/2} - \frac{\pi}{0.18}\right]g\left(\frac{\bar{y}}{\bar{\theta}}\right) \quad (6)$$

is considered.

The criterion for choosing $g(\bar{y}/\bar{\theta})$ was that it be a relatively simple function that does a reasonable job of describing the trend of experimental velocity data. The experimental data trends were investigated by solving for $g(\bar{y}/\bar{\theta})$ from Eq. (6), using experimental data for $\bar{u}^+$, $\bar{y}^+$, and $\bar{c}_f$, and plotting $g(\bar{y}/\bar{\theta})$ vs $\bar{y}/\bar{\theta}$. An example of the trends is given in Ref. 5 for favorable and highly adverse pressure gradient flows.

The analytical function used to describe the distribution of the data is taken as

$$g\left(\frac{\bar{y}}{\bar{\theta}}\right) = \tanh^{1/2}\left[a\left(\frac{\bar{y}}{\bar{\theta}}\right)^b\right] \quad (7)$$

where a and b are parameters that are constant for a given boundary-layer profile and are functions of $\bar{c}_f$, $\bar{H}$, and $\overline{Re}_\theta$. The complete velocity distribution is, therefore, given by

$$\bar{u}^+ = \frac{1}{0.09}\tan^{-1}(0.09\bar{y}^+) + \left[\left(\frac{2}{\bar{c}_f}\right)^{1/2} - \frac{\pi}{0.18}\right]\tanh^{1/2}\left[a\left(\frac{\bar{y}}{\bar{\theta}}\right)^b\right] \quad (8)$$

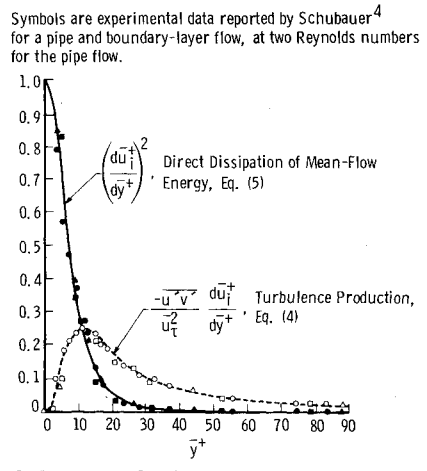

Fig. 1 Turbulence production and dissipation distributions according to Eqs. (4) and (5) and the experimental data reported by Schubauer.[4]

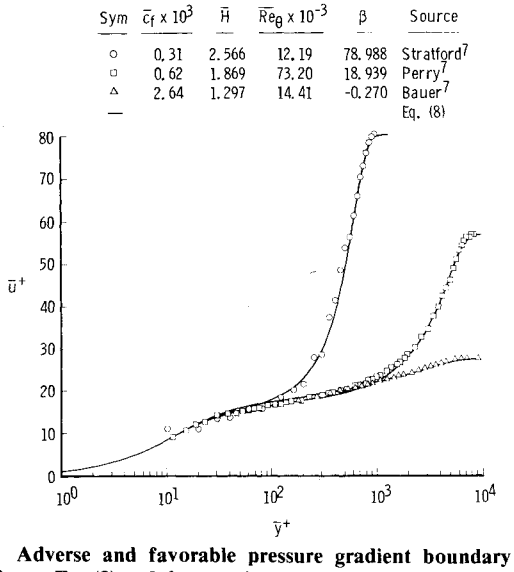

Fig. 2 Adverse and favorable pressure gradient boundary layers according to Eq. (8) and the experimental data of Stratford et al.[7]

where

$$\left(\frac{2}{\bar{c}_f}\right)^{1/2} = \bar{u}_e^+, \quad \bar{y}^+ = \frac{\overline{Re_\theta}}{\bar{u}_e^+}\frac{\bar{y}}{\bar{\theta}}, \text{ and } \frac{\bar{u}}{\bar{u}_e} = \frac{\bar{u}^+}{\bar{u}_e^+}$$

The parameters a and b were determined by satisfying the requirement that velocity profiles similar to those correlated by von Doenhoff and Tetervin[3] be recovered away from the wall in the outer variable $\bar{y}/\bar{\theta}$. The precise profiles established in Ref. 3 were not recovered, because of the fact that presumably more accurate data were obtained subsequent to the publication date (1943) of Ref. 3, and also because a Reynolds number effect on the velocity profiles was reported (see e.g., Ref. 6) subsequent to the appearance of Ref. 3. The correlations used were developed in Ref. 5 for two-dimensional planar flow and are steps 2 and 3 in Table 1. Table 1 is a summary of the solution to Eq. (8) for a and b at the two outer region match points of $\bar{y}/\bar{\theta}=2$ and 5.

Comparisons with Experimental Data

Experimental data are compared with Eq. (8) in Fig. 2 in the variables $\bar{u}^+$ and $\bar{y}^+$. The data of Perry[7] were taken in a decreasing adverse pressure gradient flow, and Stratford's data[7] were taken downstream of an abrupt onset of severe positive pressure gradient. Both Perry and Stratford's data are out of equilibrium and Stratford's data are near separation. Bauer's measurements[7] were made in water falling down a plate glass surface, and this boundary layer was near equilibrium. The agreement between Eq. (8) and the data in Fig. 2 is considered good. Note that there is little, if any, logarithmic region remaining in Stratford's profile.

Further comparisons with experimental data are given in Ref. 5 that include reattached boundary-layer data and variable pressure gradient compressible boundary-layer data. For application to compressible flow, the reader is referred to Ref. 5.

Summary

The analytical expression presented for the velocity distribution of a turbulent boundary layer was shown to be in good agreement with experimental data over the entire domain $0 \le y < \infty$. The analytical result describes experimental velocity, Reynolds stress, turbulence production, and turbulence dissipation data in the region near the wall; matches correlated velocity distributions at $\bar{y}/\bar{\theta}=2$ and 5; and gives the proper limiting velocity as $\bar{y}\to\infty$. The resulting expression gives velocity explicitly as a function of $\bar{y}$ and depends on boundary-layer properties that are explicitly defined.

Acknowledgments

The work reported herein was conducted by the Arnold Engineering Development Center (AEDC), Air Force Systems Command (AFSC). Research and analysis were done by personnel of ARO, Inc., AEDC Division, a Sverdrup Corporation Company, operating contractor for AEDC.

References

[1] Coles, D., "The Law of the Wake in the Turbulent Boundary Layer," *Journal of Fluid Mechanics*, Vol. 1, 1956, pp. 191-226.

[2] Whitfield, D.L., "Analytical, Numerical, and Experimental Results on Turbulent Boundary Layers," AEDC-TR-76-62, July 1976.

[3] von Doenhoff, A.E. and Tetervin, N., "Determination of General Relations for the Behavior of Turbulent Boundary Layers," NACA Rept. No. 772, 1943.

[4] Schubauer, G.B., "Turbulent Processes as Observed in Boundary Layer and Pipe," *Journal of Applied Physics*, Vol. 25, Feb. 1954, pp. 188-196.

[5] Whitfield, D.L., "Analytical Description of the Complete Turbulent Boundary Layer Velocity Profile," AIAA Paper 78-1158, July 1978.

[6] Thompson, B.G.J., "A New Two-Parameter Family of Mean Velocity Profiles for Incompressible Turbulent Boundary Layers on Smooth Walls," Aeronautical Research Council, London, Repts. and Memo. No. 3463, April 1965.

[7] Coles, D.E. and Hirst, E.A., ed., *Proceedings Computation of Turbulent Boundary Layers—1968 AFOSR-IFP-Stanford Conference*, Vol. II Compiled Data, Stanford Univ., Stanford, Calif.

Mass Matrix Correction Using an Incomplete Set of Measured Modes

Alex Berman*
Kaman Aerospace Corporation, Bloomfield, Conn.

Introduction

THE comparison of dynamic analysis and dynamic test data taken on a linear lightly damped structure rarely demonstrates complete or acceptable compatibility. A number of methods have been published and discussed which assume that the analytical mass matrix is correct and then modify the measured modes to achieve orthogonality.[1-7] The assumption regarding the accuracy of the mass matrix is questionable and has been briefly discussed in a recent Technical Comment.[8] The opposite approach has also been taken which assumes that the measured modes are correct and modifies the mass matrix to achieve orthogonality.[9,10] This concept has some appeal in that the resulting analytical model (including a corrected stiffness matrix, as for example in Ref. 6) will exactly predict the results obtained in the test. Other related approaches which modify analytical matrices based on a direct comparison of predictions and measurements have been published.[11,12] These approaches are outside the scope of the present discussion, however.

As a general observation, consider three sets of data: an analytical mass matrix, an analytical stiffness matrix, and an incomplete set of measured modes. It is apparent that, if any one of these sets is assumed to be exact, it is possible to correct the other two to arrive at a model which is completely compatible with the measured data.

In Ref. 9, a rather general method of correcting the mass matrix was presented which allowed the analyst to decide which elements are to be allowed to vary and to introduce confidence factors and other external linear constraints. The method presented below is less general, especially in that all elements of the matrix will change. This method, however, is considerably simpler and will require fewer computer resources. It is probably the appropriate approach for larger problems. This method uses the method of Lagrange multipliers and the derivation was inspired by the analysis presented in Ref. 6.

Analysis

M_A is an $(n\times n)$ analytical mass matrix and Φ is an $(n\times m)$ measured modal matrix. m is the number of modes and n is the number of degrees of freedom which must correspond to the measurement points on the structure and $m<n$. The measured individual modes have been normalized so that $\Phi_i{}^T M_A \Phi_i = 1$. ΔM represents changes in the mass matrix required to satisfy the orthogonality relationship:

$$\Phi^T (M_A + \Delta M)\Phi = I$$

Received April 26, 1979. Copyright © American Institute of Aeronautics and Astronautics, Inc., 1979. All rights reserved.

Index categories: Structural Dynamics; Structural Design.

*Principal Research Engineer. Member AIAA.